



HAL
open science

Optimization of the double isotope dilution

Alexandre Quemet, Sarah Baghdadi

► **To cite this version:**

Alexandre Quemet, Sarah Baghdadi. Optimization of the double isotope dilution. Journal of Analytical Atomic Spectrometry, 2021, pp.10.1039/D1JA00322D. 10.1039/D1JA00322D . cea-03471078

HAL Id: cea-03471078

<https://cea.hal.science/cea-03471078>

Submitted on 8 Dec 2021

HAL is a multi-disciplinary open access archive for the deposit and dissemination of scientific research documents, whether they are published or not. The documents may come from teaching and research institutions in France or abroad, or from public or private research centers.

L'archive ouverte pluridisciplinaire **HAL**, est destinée au dépôt et à la diffusion de documents scientifiques de niveau recherche, publiés ou non, émanant des établissements d'enseignement et de recherche français ou étrangers, des laboratoires publics ou privés.

1 **Optimization of the double isotope dilution**

2 *Alexandre Quemet¹ and Sarah Baghdadi¹*

3 ¹ *CEA, DES, ISEC, DRMC, Univ Montpellier, Marcoule, France*

4 E-mail address of the corresponding author: alexandre.quemet@cea.fr

5 **Abstract**

6 The double isotope dilution is a powerful methodology to measure accurately the ratio
7 between two isotopes of two different elements (*e.g.* ²³⁸Pu/²³⁸U, ¹⁴⁸Nd/²³⁸U or
8 ²³⁰Th/²³⁸U ratios). To obtain the lowest possible uncertainty, some parameters must be
9 optimized: the elaboration of the spike and the proportion of the spike in the sample -
10 spike mixture. A piece of code is also provided to easily calculate the optimal
11 parameters. As an example, the application of the code to ²³⁸Pu/²³⁸U and ¹⁴⁸Nd/²³⁸U
12 ratios determination in irradiated sample will be discussed.

13 **Keywords**

14 Mass spectrometry; double isotope dilution, isotope dilution

15

16 **1. Introduction**

17 Determining the ratio between two isotopes of two elements (*e.g.* $^{238}\text{Pu}/^{238}\text{U}$, $^{148}\text{Nd}/^{238}\text{U}$
18 or $^{230}\text{Th}/^{238}\text{U}$ ratios) is of prime interest in the nuclear and the geochemistry fields. One
19 of the main application in the nuclear field is the burnup monitoring of irradiated
20 samples using the $^{148}\text{Nd}/^{238}\text{U}$ ratio [1–3]. The ^{148}Nd isotope have the suitable properties
21 for burnup level examination: it is a stable fission product and requires no decay
22 correction, it is not volatile and has no volatile precursors, it is formed exclusively by
23 fission as it has a low neutron capture cross section and is not present in non-irradiated
24 samples. Other applications can be the transmutation yield determination for analytical
25 irradiation examination or to determine the capture integral cross section of different
26 isotopes [4–6]. In geochemistry, isotopes ratios like $^{230}\text{Th}/^{238}\text{U}$ or $^{226}\text{Ra}/^{238}\text{U}$ help
27 identifying and characterize the contamination sources [7–9]. It can also be useful to
28 date geological objects [10–13]. These applications require measuring these ratios with
29 the best possible accuracy (*i.e.* measurement trueness and precision).

30 Isotope dilution (ID) is the main methodology used in mass spectrometry to determine
31 accurately the mass fraction determination of an analyte in a sample, as it is a reference
32 calibration method [14–17]. The ID principle is to mix a known amount of a sample,
33 with a known isotope composition, with a spike solution containing the same analyte
34 as the sample but with a different isotope composition. This solution is called the
35 (sample–spike) mixture and its isotope ratio reflects the sample analyte mass fraction.
36 To obtain the best performance (*i.e.* the minimum mass fraction uncertainty), the
37 mixture between the sample and the spike must be prepared carefully. The ID-TIMS
38 require an optimal mixture isotope ratio which can be determined theoretically [15].
39 The mixture is then prepared to obtain a mixture isotope ratio as close as possible to the
40 theoretical one. The ratio between two isotopes of two elements is then calculated using
41 the mass fraction of the two elements determined with the ID methodology, the isotope
42 abundances and the molar masses. This method requires several gravimetric
43 preparations which can increase the uncertainties. Moreover, it can be tedious when
44 working in glove boxes or in hot cell laboratories.

45 Another existing method is the double isotope dilution (DID) method: it is used to
46 directly determine the ratio between two isotopes of two elements present in a sample,

47 with one of them used as a reference [6]. Similarly to the ID, the DID is based on the
48 addition of a spike to the sample. The spike solution must contain the same two analytes
49 as the sample with a different isotope composition. The spike can be homemade and
50 prepared from two Certified Reference Material (CRM) or a well-recognized CRM
51 provided by an official supplier (NIST, JRC-Geel or CETAMA for example) can be
52 used. The mixture isotope ratios are then measured using an accurate technique such as
53 Thermal Ionization Mass Spectrometry (TIMS) or Multi-Collector Inductively Coupled
54 Plasma Mass Spectrometry (MC-ICP-MS). The mixture isotope ratios measurements
55 helped to calculate the ratio between two isotopes of two elements in the sample. The
56 benefit of the DID compared to the ID is that it is only based on the isotope ratio
57 determination. Separation yields and weights uncertainties are not to be considered. The
58 mixture or sample dilutions can be performed volumetrically without uncertainty
59 degradation. Thus, implementing the DID is easier compared to the ID, especially when
60 the experiments are performed in glove boxes or in hot-cells. To obtain the best
61 performances for DID, some parameters like the spike solution preparation or the
62 (sample - spike) mixture must be optimized.

63 Note that the DID must not be mistaken for reverse (or two-step) ID that is used when
64 the spike is not certified. The spike material is calibrated against a well-characterized
65 assay material with natural isotope abundance [18]. The DID must not be mistaken for
66 the double spike technique. The double spike technique is a powerful method for
67 correcting the instrumental mass fractionation in mass spectrometry. It is the most
68 reliable method to obtain accurate isotope ratios of a single element [19].

69 This study aims at discussing and finding the optimal parameters for the DID. First, the
70 DID will be summarized. Then, the theoretical calculations performed to find the
71 optimal parameters will be discussed. Finally, different examples, coming from
72 samples analyzed in the laboratory, will be evaluated. To make it as easy as possible
73 for experimenters using the DID, a script written with open source software Octave is
74 provided to easily determine the optimal parameters.

75 **2. Materials and methods**

76 **2.1. Overview of the double isotope dilution methodology**

77 2.1.1. Glossary

78 A schematic of the DID is presented in Fig. 1. The goal of the DID is to measure the
79 ratio between two isotopes of two elements. Element 1 (noted E) is the reference
80 element. Isotopes of element E are ^AE and ^BE . The reference isotope of E for the sample
81 is the ^BE isotope (e.g. ^{238}U). The major isotope of the CRM used in the spike for element
82 E is ^AE (e.g. ^{233}U or ^{235}U). The second element (noted element Z) can be any element
83 of the periodic table with at least 2 isotopes. The isotopes of interest for element Z are
84 ^XZ and ^YZ . ^XZ is the major isotope of the CRM (e.g. ^{242}Pu or ^{150}Nd). ^YZ is the isotope
85 of interest for the sample (e.g. ^{238}Pu or ^{148}Nd). The “spike” term refers to the solution
86 containing E and Z elements with a known $^Y\text{Z}/^A\text{E}$ ratio. The spike can be obtained from
87 a CRM containing both elements or manufactured using two CRMs. For better clarity
88 and concision, the following nomenclature was used in the manuscript:

- 89 - T refers to the spike (or tracer). It contains both elements E and Z
- 90 - M refers to the (sample – spike) mixture
- 91 - S refers to the sample
- 92 - CRM_E refer to the CRM containing only element E
- 93 - CRM_Z refer to the CRM containing only element Z
- 94 - n is the amount in mol
- 95 - C is the amount concentration in mol g^{-1}
- 96 - $(\%A)$ refers to the ^AE isotope abundance of element E (A being the major isotope
97 of the CRM or spike)
- 98 - $(\%B)$ refers to the ^BE isotope abundance of element E (B being the reference
99 isotope of the sample)
- 100 - $(\%X)$ refers to the ^XZ isotope abundance of element Z (X being the major isotope
101 of the CRM or spike)

102 - (%Y) refers to the ^YZ isotope abundance of element Z (Y being the reference
103 isotope of the sample)

104 - *u* is the uncertainty with a coverage factor at *k* = 1

105 - *u_r* is the relative uncertainty with a coverage factor at *k* = 1

106 - *κ* is the proportion of element E in the spike solution (T)

107 - (1- *κ*) is the proportion of element Z in the spike solution (T)

108 - *λ* is the proportion of the spike solution (T) in the mixture (M)

109 2.1.2. Double isotope dilution formula

110 The (^BE/^AE)_M ratio can be calculated from the E element sample and spike amount and
111 the E element isotope abundances (Eq. (1), Fig. 1).

$$\left(\frac{^B E}{^A E}\right)_M = \frac{n(E)_S \cdot (\%B)_S + n(E)_T \cdot (\%B)_T}{n(E)_S \cdot (\%A)_S + n(E)_T \cdot (\%A)_T} \quad (1)$$

$$(\%A)_S = (\%B)_S \cdot \left(\frac{^A E}{^B E}\right)_S \quad (2)$$

$$(\%B)_T = (\%A)_T \cdot \left(\frac{^B E}{^A E}\right)_T \quad (3)$$

112 Combining Eq. (1), (2) and (3) leads to Eq. (4).

$$\left(\frac{^B E}{^A E}\right)_M = \frac{n(E)_S \cdot (\%B)_S + n(E)_T \cdot \left(\frac{^B E}{^A E}\right)_T \cdot (\%A)_T}{n(E)_S \cdot (\%B)_S \cdot \left(\frac{^A E}{^B E}\right)_S + n(E)_T \cdot (\%A)_T} \quad (4)$$

113 Rearranging Eq. (4) leads to Eq. (5).

$$n(E)_S \cdot (\%B)_S = n(E)_T \cdot (\%A)_T \cdot \frac{\left(\left(\frac{^B E}{^A E}\right)_M - \left(\frac{^B E}{^A E}\right)_T\right)}{\left(1 - \left(\frac{^B E}{^A E}\right)_M \cdot \left(\frac{^A E}{^B E}\right)_S\right)} \quad (5)$$

114 The same equation as Eq. (5) can be obtained for element Z (Eq. (6)).

$$n(Z)_S \cdot (\%Y)_S = n(Z)_T \cdot (\%X)_T \cdot \frac{\left(\left(\frac{YZ}{XZ} \right)_M - \left(\frac{YZ}{XZ} \right)_T \right)}{\left(1 - \left(\frac{YZ}{XZ} \right)_M \cdot \left(\frac{XZ}{YZ} \right)_S \right)} \quad (6)$$

115 Dividing Eq. (6) by Eq. (5) leads to the $(YZ/BE)_S$ ratio and the DID formula (Eq. (7)).

$$\left(\frac{YZ}{BE} \right)_S = \left(\frac{XZ}{AE} \right)_T \cdot \frac{\left(\left(\frac{YZ}{XZ} \right)_M - \left(\frac{YZ}{XZ} \right)_T \right) \cdot \left(1 - \left(\frac{BE}{AE} \right)_M \cdot \left(\frac{AE}{BE} \right)_S \right)}{\left(\left(\frac{BE}{AE} \right)_M - \left(\frac{BE}{AE} \right)_T \right) \cdot \left(1 - \left(\frac{YZ}{XZ} \right)_M \cdot \left(\frac{XZ}{YZ} \right)_S \right)} \quad (7)$$

116 2.1.3. Uncertainty estimation

117 The $(YZ/BE)_S$ ratio uncertainty ($u[(YZ/BE)_S]$, $k = 1$, Eq. (8)) was estimated by combining
 118 the uncertainties from each term of the DID equation (Eq. (7)) [20]. The terms of Eq. (7)
 119 were considered as not correlated, so no covariance terms are needed.

$$\begin{aligned}
u^2 \left(\left(\frac{Y Z}{B E} \right)_S \right) &= \left(\frac{\left(\left(\frac{Y Z}{X Z} \right)_M - \left(\frac{Y Z}{X Z} \right)_T \right) \cdot \left(\left(\frac{B E}{A E} \right)_M \cdot \left(\frac{A E}{B E} \right)_S - 1 \right)}{\left(\left(\frac{B E}{A E} \right)_M - \left(\frac{B E}{A E} \right)_T \right) \cdot \left(\left(\frac{Y Z}{X Z} \right)_M \cdot \left(\frac{X Z}{Y Z} \right)_S - 1 \right)} \right)^2 \cdot u^2 \left(\left(\frac{X Z}{A E} \right)_T \right) \\
&+ \left(- \left(\frac{X Z}{A E} \right)_T \cdot \frac{\left(\left(\frac{B E}{A E} \right)_M \cdot \left(\frac{A E}{B E} \right)_S - 1 \right)}{\left(\left(\frac{B E}{A E} \right)_M - \left(\frac{B E}{A E} \right)_T \right) \cdot \left(\left(\frac{Y Z}{X Z} \right)_M \cdot \left(\frac{X Z}{Y Z} \right)_S - 1 \right)} \right)^2 \cdot u^2 \left(\left(\frac{Y Z}{X Z} \right)_T \right) \\
&+ \left(\left(\frac{X Z}{A E} \right)_T \cdot \frac{\left(\left(\frac{Y Z}{X Z} \right)_M - \left(\frac{Y Z}{X Z} \right)_T \right) \cdot \left(\left(\frac{B E}{A E} \right)_M \cdot \left(\frac{A E}{B E} \right)_S - 1 \right)}{\left(\left(\frac{B E}{A E} \right)_M - \left(\frac{B E}{A E} \right)_T \right)^2 \cdot \left(\left(\frac{Y Z}{X Z} \right)_M \cdot \left(\frac{X Z}{Y Z} \right)_S - 1 \right)} \right)^2 \cdot u^2 \left(\left(\frac{B E}{A E} \right)_T \right) \\
&+ \left(- \left(\frac{X Z}{A E} \right)_T \cdot \left(\frac{Y Z}{X Z} \right)_M \cdot \frac{\left(\left(\frac{Y Z}{X Z} \right)_M - \left(\frac{Y Z}{X Z} \right)_T \right) \cdot \left(\left(\frac{B E}{A E} \right)_M \cdot \left(\frac{A E}{B E} \right)_S - 1 \right)}{\left(\left(\frac{B E}{A E} \right)_M - \left(\frac{B E}{A E} \right)_T \right)^2 \cdot \left(\left(\frac{Y Z}{X Z} \right)_M \cdot \left(\frac{X Z}{Y Z} \right)_S - 1 \right)} \right)^2 \\
&\cdot u^2 \left(\left(\frac{X Z}{Y Z} \right)_S \right) \\
&+ \left(\left(\frac{X Z}{A E} \right)_T \cdot \left(\frac{B E}{A E} \right)_M \cdot \frac{\left(\left(\frac{Y Z}{X Z} \right)_M - \left(\frac{Y Z}{X Z} \right)_T \right)}{\left(\left(\frac{B E}{A E} \right)_M - \left(\frac{B E}{A E} \right)_T \right) \cdot \left(\left(\frac{Y Z}{X Z} \right)_M \cdot \left(\frac{X Z}{Y Z} \right)_S - 1 \right)} \right)^2 \\
&\cdot u^2 \left(\left(\frac{A E}{B E} \right)_S \right) + \left(- \left(\frac{X Z}{A E} \right)_T \cdot \frac{\left(\left(\frac{Y Z}{X Z} \right)_M - \left(\frac{Y Z}{X Z} \right)_T \right) \cdot \left(1 - \left(\frac{B E}{A E} \right)_T \cdot \left(\frac{A E}{B E} \right)_S \right)}{\left(\left(\frac{B E}{A E} \right)_M - \left(\frac{B E}{A E} \right)_T \right)^2 \cdot \left(\left(\frac{Y Z}{X Z} \right)_M \cdot \left(\frac{X Z}{Y Z} \right)_S - 1 \right)} \right)^2 \\
&\cdot u^2 \left(\left(\frac{B E}{A E} \right)_M \right) + \left(\left(\frac{X Z}{A E} \right)_T \cdot \frac{\left(\left(\frac{Y Z}{X Z} \right)_T \cdot \left(\frac{X Z}{Y Z} \right)_S - 1 \right) \cdot \left(\left(\frac{B E}{A E} \right)_M \cdot \left(\frac{A E}{B E} \right)_S - 1 \right)}{\left(\left(\frac{B E}{A E} \right)_M - \left(\frac{B E}{A E} \right)_T \right) \cdot \left(\left(\frac{Y Z}{X Z} \right)_M \cdot \left(\frac{X Z}{Y Z} \right)_S - 1 \right)^2} \right)^2 \\
&\cdot u^2 \left(\left(\frac{Y Z}{X Z} \right)_M \right)
\end{aligned} \tag{8}$$

120 2.2. Optimization of the double isotope dilution methodology

121 The DID methodology requires a parameters optimization to obtain the most accurate
122 results: *i.e.* the minimal $(Y Z/B E)_S$ relative uncertainty. Two different optimizations can
123 be performed. The first optimization is needed if the spike solution (T) must be prepared
124 using 2 CRMs. In this case, it is possible to optimize the proportion of each element in
125 the spike solution (T) (κ parameter for element E and $(1 - \kappa)$ for element Z) and the
126 proportion of the spike solution (T) in the mixture (M) (λ parameter). The second one
127 is if the spike solution (T) containing both elements is already prepared or using a CRM
128 solution commercially available. In this case the only parameter which can be optimized
129 is the proportion of the spike solution (T) in the mixture (λ parameter).

130 *2.2.1. Simultaneous optimization of λ and κ parameters for a spike*
 131 *solution prepared from two CRMs*

132 The $(^{XZ}/^AE)_T$ ratio can be calculated as a function of the proportion of E and Z CRM in
 133 the spike (κ and $(1-\kappa)$ parameters), amount concentrations and isotope abundances
 134 (Eq. (9)). Please note $(\%A)$, $(\%B)$, $(\%X)$ and $(\%Y)$ are the same in the CRM and in the
 135 spike, and will be referred to as $(\%A)_T$, $(\%B)_T$, $(\%X)_T$ and $(\%Y)_T$, respectively.

136

$$\left(\frac{^{XZ}}{^AE}\right)_T = \frac{(1 - \kappa) \cdot C(Z)_{CRM_Z} \cdot (\%X)_T}{\kappa \cdot C(E)_{CRM_E} \cdot (\%A)_T} \quad (9)$$

137 The $(^{BE}/^AE)_M$ ratio can be calculated as a function of the proportion of E CRM in the spike
 138 (κ parameter), the proportion of spike in the mixture (λ parameter), amount
 139 concentrations and isotope abundances (Eq. (10)).

$$\left(\frac{^{BE}}{^AE}\right)_M = \frac{\lambda \cdot \kappa \cdot C(E)_{CRM_E} \cdot (\%B)_T + (1 - \lambda) \cdot C(E)_S \cdot (\%B)_S}{\lambda \cdot \kappa \cdot C(E)_{CRM_E} \cdot (\%A)_T + (1 - \lambda) \cdot C(E)_S \cdot (\%A)_S} \quad (10)$$

140 The $(^{YZ}/^XZ)_M$ ratio can be calculated by the same way using Eq. (11).

$$\left(\frac{^{YZ}}{^XZ}\right)_M = \frac{\lambda \cdot (1 - \kappa) \cdot C(Z)_{CRM_Z} \cdot (\%Y)_T + (1 - \lambda) \cdot C(Z)_S \cdot (\%Y)_S}{\lambda \cdot (1 - \kappa) \cdot C(Z)_{CRM_Z} \cdot (\%X)_T + (1 - \lambda) \cdot C(Z)_S \cdot (\%X)_S} \quad (11)$$

141 By introducing Eqs. (9), (10) and (11) in Eqs. (7) and (8), the $(^{YZ}/^{BE})_S$ ratio relative
 142 uncertainty ($u_r[(^{YZ}/^{BE})_S]$) can be expressed as a function of λ and κ (Eq. (12)).

$$u_r\left(\left(\frac{^{YZ}}{^{BE}}\right)_S\right) = f(\lambda, \kappa) \quad (12)$$

143 Finding the λ and κ optimal parameters is simply a matter of locating the minimal
 144 relative uncertainty of the $(^{YZ}/^{BE})_S$ ratio. It helps obtaining the most accurate result.
 145 The $(^{BE}/^AE)_M$ and $(^{YZ}/^XZ)_M$ optimal mixture isotope ratios are then calculated by
 146 introducing optimal λ and κ parameters in Eqs. (10) and (11).

147 It is possible to plot the function described in Eq. (12) to study the variation of the
 148 relative uncertainty as a function of λ and κ . An example of this plot, hereafter referred
 149 to as a contour plot, is shown in Fig. 2. The contours are spaced out with intervals of

150 1 % of the optimal relative uncertainty. The plot is cut off so that only contours within
 151 20 % of the minimal error are shown. The contour plot is useful to show how robust the
 152 optimal parameters are. In fact, the sample amount concentration ($c(E)_S$) and $c(Z)_S$ are
 153 generally not accurately known. It can be provided by different sources: neutronic
 154 simulation code, fast analytical technic like UV/Vis spectrometry or L-line X-ray
 155 fluorescence or estimated using the results from previous experiments. It is difficult to
 156 mix the sample and the spike with the exact and optimal proportions. So, it is important
 157 to understand how the error of the relative uncertainty varies around the λ and κ optimal
 158 parameters.

159 *2.2.2. Optimization of the λ parameter for a spike solution already*
 160 *prepared or commercially available*

161 If the homemade spike is already prepared or if using a commercially available spike,
 162 the κ parameter is a fixed characteristic of the spike and does not need to be optimized:
 163 in others words the $(^XZ/^AE)_T$ ratio is known. The λ parameter can only be optimized to
 164 obtain the minimal $(^YZ/^BE)_S$ ratio relative uncertainty.

165 The $(^BE/^AE)_M$ ratio can be calculated depending on E and Z element amount
 166 concentration in the spike, the proportion of spike in the mixture (λ parameter), sample
 167 amount and isotope abundances (Eq. (13)).

$$\left(\frac{^BE}{^AE}\right)_M = \frac{\lambda \cdot C(E)_T \cdot (\%B)_T + (1 - \lambda) \cdot C(E)_S \cdot (\%B)_S}{\lambda \cdot C(E)_T \cdot (\%A)_T + (1 - \lambda) \cdot C(E)_S \cdot (\%A)_S} \quad (13)$$

168 In the same way, the $(^YZ/^XZ)_M$ ratio can be calculated (Eq. (14)).

$$\left(\frac{^YZ}{^XZ}\right)_M = \frac{\lambda \cdot C(Z)_T \cdot (\%Y)_T + (1 - \lambda) \cdot C(Z)_S \cdot (Y)_S}{\lambda \cdot C(Z)_T \cdot (\%X)_T + (1 - \lambda) \cdot n(Z)_S \cdot (\%X)_S} \quad (14)$$

169 By introducing Eq. (13) and (14) in Eq. (7) and (8), the $(^YZ/^BE)_S$ ratio relative
 170 uncertainty as a function of λ is calculated (Eq. (15)).

$$u_r \left(\left(\frac{^YZ}{^BE} \right)_S \right) = f(\lambda) \quad (15)$$

171 Finding the λ optimal value is simply a matter of locating the minimal relative
172 uncertainty of the sample ${}^Y Z/{}^B E$ ratio. The $({}^B E/{}^A E)_M$ and $({}^Y Z/{}^X Z)_M$ optimal ratio are
173 then calculated by introducing the optimal λ in Eq. (13) and (14). To understand how
174 the error varies around the λ optimal value, the error of the relative uncertainty as a
175 function of λ can be drawn.

176 2.3. Script

177 All the calculation were implemented in a script written with the open source software
178 Octave [21], version 5.1.0. To start the script, unzip the “double_ID_optimization.zip”
179 file available in the supplementary materials. Start Octave software and set the browser
180 directory to the appropriate folder where the unzipped folder is located. Starting the
181 script is performed by typing “startup_DID” in the Octave command window. Then,
182 the script allows to select which parameters need to optimized: simultaneous
183 optimization of λ and κ parameters or optimization of the λ parameter. Then, all
184 parameters, including the choice of elements and isotopes, must be selected. The default
185 parameters can be modified in the “private/default_value_data_double_ID.m” file.
186 Once the calculation is complete, the optimal parameters, including the optimal mixture
187 isotope ratios, are displayed in the Octave command windows. The plot are also
188 displayed. The plot can be saved as a 8 cm \times 8 cm “.png” file. The results and the raw
189 data can be saved in a “.txt” file.

190 2.4. Experimental

191 As concrete examples, experiments performed on samples from the DIAMINO
192 irradiation were considered in details [4, 22]. The DIAMINO irradiation was an
193 analytical irradiation experiment performed on UAmO₂ discs to study their behaviors
194 under irradiation, to determine the americium transmutation yield and to study the
195 influence of the microstructure on the gas release as a function of temperature. Among
196 the determinations, ${}^{238}\text{Pu}/{}^{238}\text{U}$, ${}^{241}\text{Am}/{}^{238}\text{U}$ and ${}^{148}\text{Nd}/{}^{238}\text{U}$ ratios were of prime interest.
197 In these examples, ${}^{238}\text{Pu}/{}^{238}\text{U}$ and ${}^{148}\text{Nd}/{}^{238}\text{U}$ ratios were investigated in more details.
198 Thus, element Z can be Pu and Nd alternatively. The first element E was chosen as

199 uranium as it is usually used as reference in the nuclear field. Its reference isotope is
200 ${}^B E = {}^{238}\text{U}$.

201 All theoretical investigations were performed on the same sample (DIAMINO sample
202 [4, 22]). The characteristics of the sample have been summarized in Table 1. The
203 isotope ratios, abundances and uncertainties of the sample were determined in previous
204 studies [4, 22]. The U and Pu amount concentration of the sample were estimated using
205 a L-line X-ray fluorescence analysis located in a shielded line [23]. It is a non-
206 destructive, non-invasive and relatively fast technique giving the actinide amount
207 concentration with an uncertainty of about 10 %. This measurement is important to
208 obtain a reliable estimation of the U and Pu amount concentration in the sample before
209 implementing the DID. The Nd amount concentration was estimated using a neutronic
210 simulation code as Nd cannot be measure using L-line X-ray fluorescence analysis.

211 The mixture isotope ratios relative uncertainties ($u_r[({}^B E/{}^A E)_M]$ and $u_r[({}^Y Z/{}^X Z)_M]$) were
212 set at 0.07% ($k = 1$), corresponding to the International Target Value (ITV) for a
213 ${}^{238}\text{U}/{}^{235}\text{U}$ isotope ratio of about 1 [24].

214 **3. Results and discussion**

215 **3.1. Simultaneous optimization of λ and κ parameters**

216 For such case, κ is plotted versus λ , and a contour plot is presented with each line
217 representing a 1 % variation of the minimal relative uncertainty.

218 *3.1.1. ${}^{238}\text{Pu}/{}^{238}\text{U}$ ratio determination*

219 In the first case, the spike is manufactured from two uranium and plutonium CRM. The
220 reference uranium and plutonium isotope of the sample is ${}^{238}\text{U}$ (*i.e.* ${}^B E = {}^{238}\text{U}$) and ${}^{238}\text{Pu}$
221 (*i.e.* ${}^Y Z = {}^{238}\text{Pu}$), respectively. The natural choice to prepare the uranium spike is a CRM
222 enriched with ${}^{233}\text{U}$ or ${}^{235}\text{U}$ isotope (*i.e.* ${}^A E = {}^{235}\text{U}$ or ${}^{233}\text{U}$). For plutonium, a CRM
223 enriched with ${}^{242}\text{Pu}$ isotope is a good choice to prepare the spike (*i.e.* ${}^X Z = {}^{242}\text{Pu}$).

224 *3.1.1.1. Solutions enriched with ${}^{235}\text{U}$ and ${}^{242}\text{Pu}$ isotopes*

225 In this first example, the U CRM, enriched in ^{235}U (*i.e.* $^{\text{A}}\text{E} = ^{235}\text{U}$), was the IRMM 054
226 CRM provided by the Joint Research Centre of the European Commission (EC-JRC).
227 This U CRM was diluted gravimetrically to obtain a uranium mass fraction near
228 $10\ \mu\text{g g}^{-1}$. The Pu CRM, enriched in ^{242}Pu isotope (*i.e.* $^{\text{X}}\text{Z} = ^{242}\text{Pu}$), was the IRMM
229 049d CRM provided by EC-JRC. This Pu material was diluted gravimetrically to obtain
230 a plutonium mass fraction near $5\ \mu\text{g g}^{-1}$. The characteristics of the CRM, with the
231 appropriate notation, are summarized by example 1 in Table 1. The optimal λ and κ
232 parameters were 0.84 and 0.30, respectively. This corresponds to $(^{\text{B}}\text{E}/^{\text{A}}\text{E})_{\text{M}}$ and
233 $(^{\text{Y}}\text{Z}/^{\text{X}}\text{Z})_{\text{M}}$ ratios measured at 3.49 and 0.0769, respectively. The contour plot is
234 represented in Fig. 2. In this example, the optimal parameters are quite robust as the
235 relative uncertainty surface is flat: there are a wide range of λ and κ values that are
236 within 1 % of the minimal relative uncertainty. It is easy to manufacture the spike and
237 the mixture without the risk to lose the measurement accuracy. The minimal relative
238 uncertainty was estimated to 0.17 % ($k = 1$). This uncertainty corresponds to the
239 uncertainty linked to the DID uncertainty (Eq. (8)) and does not take into account the
240 repeatability.

241 3.1.1.2. Solutions enriched with ^{233}U and ^{242}Pu isotopes

242 As second example the uranium CRM used was a CRM enriched in ^{233}U isotope (*i.e.*
243 $^{\text{A}}\text{E} = ^{233}\text{U}$): the IRMM-051 CRM. The CRM characteristics for example 2 are
244 summarized in Table 1. All the other parameters are the same as in example 1 (Pu CRM
245 and sample characteristics). Using a uranium CRM enriched in ^{233}U isotope is
246 interesting as the sample generally contains no ^{233}U isotope: $(\%A)_s = 0$ and $u(AB_s) = 0$.
247 The optimal λ and κ parameters were calculated using the data in example 2 in Table 1.
248 However, in such case, the simultaneous optimization of λ and κ cannot work for
249 mathematical reasons. Indeed, the κ parameter approaches 0, which makes no sense: it
250 is impossible to compute the $(^{\text{Y}}\text{Z}/^{\text{B}}\text{E})_s$ ratio with a spike containing no U element.
251 However, the plot in Fig. 3, helps finding the optimal λ and κ parameters. The surface
252 where the relative uncertainty is within 1 % of the minimal relative uncertainty is
253 relatively flat: in this central surface, the relative uncertainty is between 0.1380 % and
254 0.1394 % ($k = 1$). Graphically, it exists a lot of λ and κ parameters pairs for the best
255 conditions: one pair, presented in Fig. 3, could be $\lambda = 0.8$ and $\kappa = 0.2$. Thus, when the

256 major isotope of a spike is not present in the sample, the λ and κ optimal parameters
257 can be determined graphically.

258 3.1.2. $^{148}\text{Nd}/^{238}\text{U}$ ratio determination

259 In this example, the optimal parameters for the determination of the $^{148}\text{Nd}/^{238}\text{U}$ ratio
260 were studied (example 3 in Table 1). The laboratory has already prepared a homemade
261 characterized Nd material [4]: this Nd material solution was prepared by dissolving a
262 ^{150}Nd enriched (95%) non-radioactive neodymium oxide powder in 3 mol L⁻¹ HNO₃.
263 The Nd mass fraction of the Nd material is about 7.5 $\mu\text{g g}^{-1}$ ($c(Z_T) = 0.0499 \times 10^{-6}$
264 mol g⁻¹). The U CRM, enriched in ^{235}U isotope, is the IRMM 054 CRM. The
265 characteristics of the material and the sample are summarized in example 3 in Table 1.

266 The optimal λ and κ parameters were 0.59 and 0.994, respectively. The optimal
267 parameters indicates that the spike must contain mostly U (only 0.06 % of Nd material
268 in the spike). The contour plot is represented in Fig. 4.a. In this example, the optimal
269 values is not robust as the relative uncertainty surface is not flat. It exist a small region
270 around the κ and λ values to obtain the minimal uncertainty. A small error on the spike
271 preparation will have a large impact on the relative uncertainty. In this case, diluting
272 the Nd material would help obtaining more robust parameters.

273 So, the λ and κ parameters were optimized again using a Nd material diluted 100-fold:
274 the Nd mass fraction is about 0.075 $\mu\text{g g}^{-1}$ ($c(Z_T) = 0.0499 \times 10^{-8}$ mol g⁻¹). All of the
275 other parameters were unchanged (example 3 in Table 1). The optimal λ and κ
276 parameters were calculated and are 0.69 and 0.61, respectively. The contour plot is
277 represented in Fig. 4.b. The optimum is now robust as the relative uncertainty surface
278 is flat: there are a wide range of λ and κ values that are within 1 % of the minimal
279 relative uncertainty. It is now easier to mix the U and Nd materials to obtain the
280 appropriate spike. With these optimal parameters, the $(^{\text{B}}\text{E}/^{\text{A}}\text{E})_{\text{M}}$ and $(^{\text{Y}}\text{Z}/^{\text{X}}\text{Z})_{\text{M}}$ mixture
281 ratio were 4.10 and 0.0117, respectively. The minimal uncertainty was estimated to
282 0.30 % ($k = 1$).

283 3.2. Optimization of the λ parameter

284 In this example a spike enriched in both elements that was already prepared or using a
285 CRM is used (example 4 in Table 1). The IRMM 046c CRM, provided by EC-JRC was
286 used in this example. It is a spike solution enriched in both ^{233}U and ^{242}Pu isotopes.
287 Uranium and plutonium amount concentrations and isotope abundances of the spike are
288 certified (see Table 1): that means the κ parameter cannot be optimized and only the λ
289 parameter can in such case. Thus, the error for the $^{238}\text{Pu}/^{238}\text{U}$ ratio relative uncertainty
290 as a function of λ is plotted.

291 In this example, the minimal relative uncertainty was found for $\lambda = 0.14$. The minimal
292 uncertainty was estimated to 0.11 % ($k = 1$). This corresponds to $(^{\text{B}}\text{E}/^{\text{A}}\text{E})_{\text{M}}$ and
293 $(^{\text{X}}\text{Z}/^{\text{Y}}\text{Z})_{\text{M}}$ ratios measured at 0.288 and 0.180, respectively. The error for the $^{238}\text{Pu}/^{238}\text{U}$
294 ratio relative uncertainty as a function of λ is shown in Fig. 5.a. In this theoretical study,
295 the relative uncertainty is almost stable around the optimal λ parameter but only for λ
296 values higher than the λ optimal parameter. For λ values lower than the optimal λ
297 parameter, the relative uncertainty increases rapidly. As the uranium and plutonium
298 amount concentration is generally not known accurately, there is a high risk to degrade
299 the accuracy measurement when performing the sample spike mixture. As the dilution
300 have no impact on the $(^{\text{X}}\text{Z}/^{\text{A}}\text{E})_{\text{T}}$ ratio uncertainty, it will be interesting to dilute the spike
301 to obtain a more robust optimal λ parameter.

302 The λ parameter was optimized using the IRMM-046c CRM diluted 10-fold:
303 $c(E_{\text{T}}) = 4.4742 \times 10^{-7} \text{ mol g}^{-1}$ and $c(Z_{\text{T}}) = 0.37519 \times 10^{-7} \text{ mol g}^{-1}$. All the others
304 parameters were the same as example 4 in Table 1: similarly, the $^{\text{Y}}\text{Z}/^{\text{A}}\text{E}$ ratio of the
305 spike remains constant whatever the dilution factor. The optimal λ parameter is now
306 equal to 0.62. As expected, the minimal relative uncertainty remains constant (0.11 %, $k = 1$)
307 as the dilution does not affect the isotope ratio. The error for the relative
308 uncertainty as a function of λ is shown in Fig. 5.b. The λ parameter is now more robust:
309 the relative uncertainty is stable around the optimal λ parameter. There are a wide range
310 of λ values corresponding to the minimal relative uncertainty.

311 **4. Conclusion**

312 The DID is a powerful method to determine two isotopes ratio of two elements present
313 in a sample, with one of them used as a reference. As it is only based on isotope ratio

314 measurement, accurate measurements can be obtained. To obtain the best performance,
315 the parameters must be set carefully, especially the spike production and the (sample –
316 spike) mixture. This work comes along with a piece of code that can be found in the
317 supplementary material, to easily calculate the optimal parameters. The source code is
318 freely available and can be modified if needed by individual users.

319

320

322 Table 1: Parameters used for the theoretical study to find the optimal parameters of
 323 the DID. The relative uncertainty are expressed with a coverage factor at $k = 1$

Example	1	2	3	4
Ratio of interest	$^{238}\text{Pu}/^{238}\text{U}$	$^{238}\text{Pu}/^{238}\text{U}$	$^{148}\text{Nd}/^{238}\text{U}$	$^{238}\text{Pu}/^{238}\text{U}$
Element 1 (E)	U	U	U	U
Element 2 (Z)	Pu	Pu	Nd	Pu
$^{\text{A}}\text{E}$ isotope (spike major isotope)	^{235}U	^{233}U	^{235}U	^{233}U
$^{\text{B}}\text{E}$ isotope (sample reference isotope)	^{238}U	^{238}U	^{238}U	^{238}U
$^{\text{X}}\text{Z}$ isotope (spike major isotope)	^{242}Pu	^{242}Pu	^{150}Nd	^{242}Pu
$^{\text{Y}}\text{Z}$ isotope (sample reference isotope)	^{238}Pu	^{238}Pu	^{148}Nd	^{238}Pu
CRM	U: IRMM 054 Pu: IRMM 49d	U: IRMM 051 Pu: IRMM 49d	U: IRMM 054 Nd: ^{150}Nd material	IRMM 46c
$(\%B)_T$	5.4102 %	0.8042 %	5.4102 %	0.2099 %
$(\%A)_T$	93.176 %	98.0430 %	93.176 %	99.763 %
$C(E)_{\text{CRM or } T}$	0.0404×10^{-6}	0.10303×10^{-6}	0.0404×10^{-6}	4.4742×10^{-6}
$u_r \left(\left(\frac{^{\text{B}}\text{E}}{^{\text{A}}\text{E}} \right)_T \right)$	0.0300 %	0.122 %	0.0300 %	0.000927 %
$(\%Y)_T$	0.50446 %	0.50446 %	0.93850 %	0.50446 %
$(\%X)_T$	94.622 %	94.622 %	94.745 %	94.622 %
$C(Z)_{\text{CRM or } T}$	0.0183×10^{-6}	0.0183×10^{-6}	0.0499×10^{-6}	0.37519×10^{-6}
$u_r \left(\left(\frac{^{\text{Y}}\text{Z}}{^{\text{X}}\text{Z}} \right)_T \right)$	0.0646 %	0.0646 %	0.170 %	0.00204 %
$u_r \left(\left(\frac{^{\text{X}}\text{Z}}{^{\text{A}}\text{E}} \right)_T \right)$	0.136 %	0.0924 %	0.282 %	0.0227 %
$(\%B)_S$	99.310 %	99.310 %	99.310 %	99.310 %
$(\%A)_S$	0.45640 %	0	0.45640 %	0
$C(E)_S$	0.209×10^{-6}	0.209×10^{-6}	0.209×10^{-6}	0.209×10^{-6}
$u_r \left(\left(\frac{^{\text{A}}\text{E}}{^{\text{B}}\text{E}} \right)_S \right)$	0.138 %	0	0.138 %	0
$(\%Y)_S$	74.010 %	74.010 %	10.447 %	74.010 %
$(\%X)_S$	15.745 %	15.745 %	6.308 %	15.745 %
$C(Z)_S$	0.0141×10^{-6}	0.0141×10^{-6}	0.000569×10^{-6}	0.0141×10^{-6}
$u_r \left(\left(\frac{^{\text{X}}\text{Z}}{^{\text{Y}}\text{Z}} \right)_S \right)$	0.0994 %	0.0994 %	0.261 %	0.0994 %

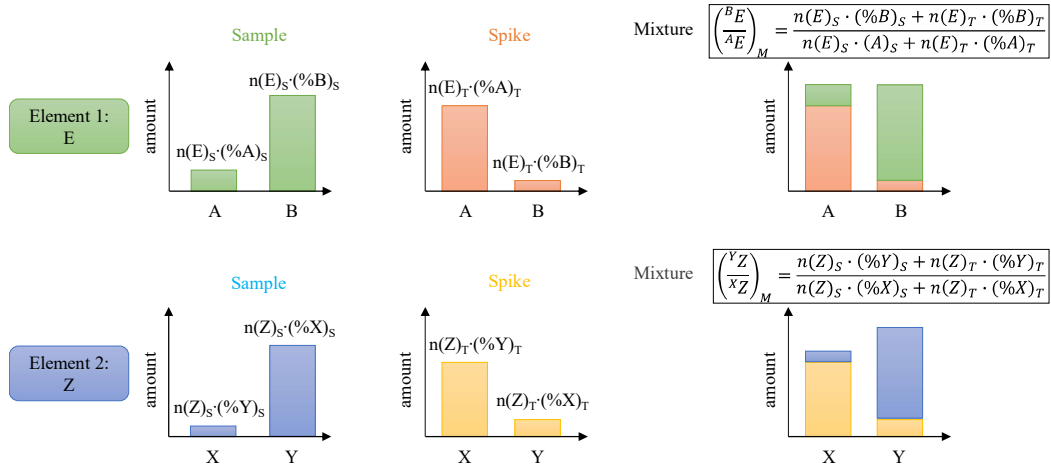
$u_r \left(\left(\frac{B}{A} \right)_M \right)$	0.07 %	0.07 %	0.07 %	0.07 %
$u_r \left(\left(\frac{Y}{X} \right)_M \right)$	0.07 %	0.07 %	0.07 %	0.07 %

324

325

Figure

326

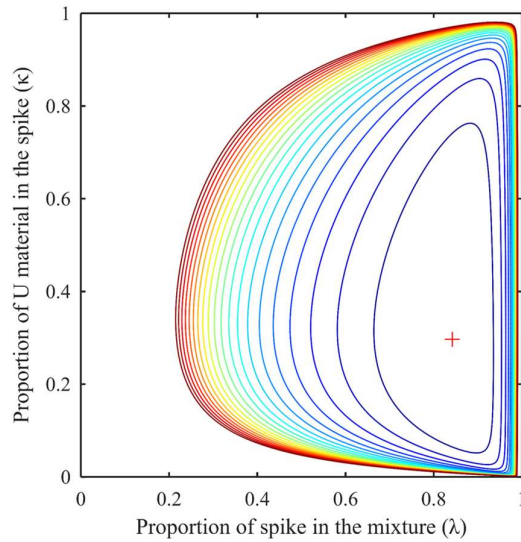


327

328

Fig. 1: Schematics of the DID methodology

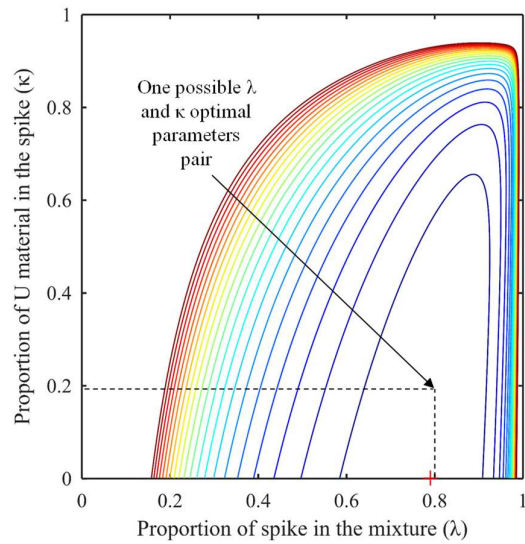
329



330

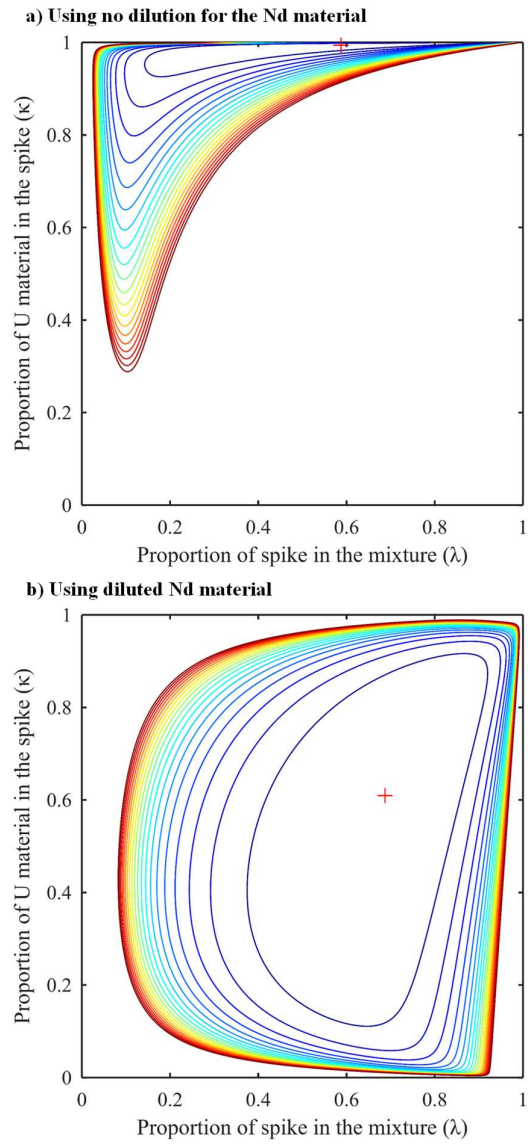
331 Fig. 2: Contour plot of error for the relative uncertainty of the sample $^{238}\text{Pu}/^{238}\text{U}$ ratio
 332 using U (IRMM-054) and Pu (IRMM-049d) CRM (example 1 in Table 1). The
 333 optimum is marked by the cross. The plot is cut off so that only contours within 20 %
 334 of the minimal error are shown. The contours are spaced out with intervals of 1 % of
 335 the minimal error

336



338

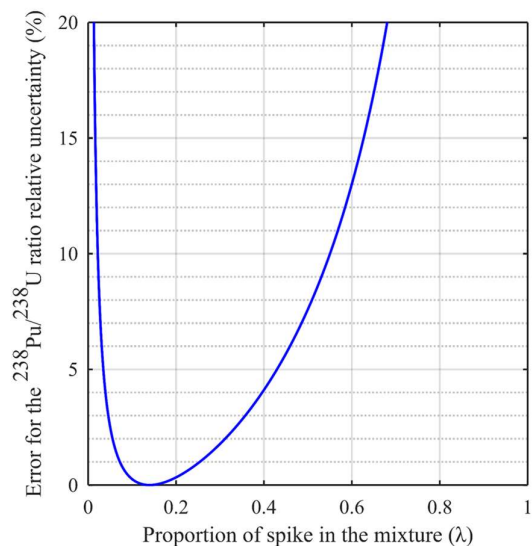
339 Fig. 3: Contour plot of error for the relative uncertainty of the sample $^{238}\text{Pu}/^{238}\text{U}$ ratio
 340 using U (IRMM-051) and Pu (IRMM-49d) CRM (example 2 in Table 1). The
 341 optimum is marked by the cross. The plot is cut off so that only contours within 20 %
 342 of the minimal error are shown. The contours are spaced out with intervals of 1 % of
 343 the minimal error



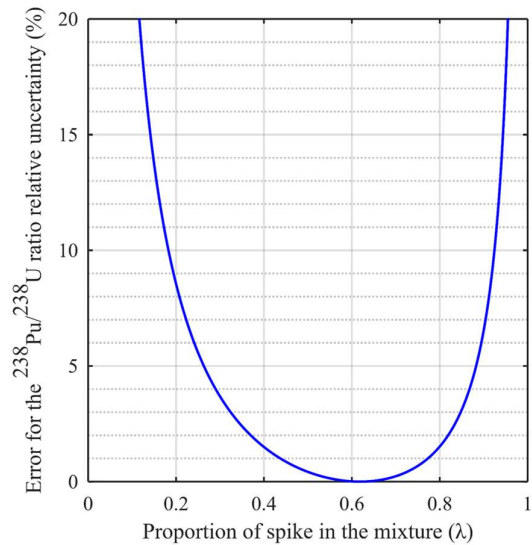
344

345 Fig. 4: Contour plot of error for the relative uncertainty of the sample $^{148}\text{Nd}/^{238}\text{U}$ ratio
 346 using U CRM (IRMM 054) and no diluted (a) and diluted (b) Nd material (example 3
 347 in Table 1). The plot is cut off so that only contours within 20 % of the minimal error
 348 are shown. The contours are spaced out with intervals of 1 % of the minimal error

a) Using IRMM-046c CRM without dilution



b) Using IRMM-046c CRM diluted 10 times



349

350 Fig. 5: Error for the $^{238}\text{Pu}/^{238}\text{U}$ ratio relative uncertainty (% , $k = 1$) as a function of λ
351 parameter using the IRMM-046c CRM without dilution (a) and diluted 10-fold (b)

352

353

354

355

356

References

- 357 1. Bachhav M, Gan J, Keiser D, Giglio J, Jädernäs D, Leenaers A, Van den
358 Berghe S (2020) A novel approach to determine the local burnup in irradiated
359 fuels using Atom Probe Tomography (APT). *J Nucl Mater* 528:.
360 <https://doi.org/10.1016/j.jnucmat.2019.151853>
- 361 2. Devida C, Betti M, Peerani P, Toscano EH, Goll W (2004) Quantitative
362 Burnup Determination: A Comparison of Different Experimental Methods. In:
363 “HOTLAB” Plenary Meeting. Halden, Norway, pp 106–113
- 364 3. Wolf SF, Bowers DL, Cunnane JC (2005) Analysis of high burnup spent
365 nuclear fuel by ICP-MS. *J Radioanal Nucl Chem* 263:581–586.
366 <https://doi.org/10.1007/s10967-005-0627-7>
- 367 4. Quemet A, Buravand E, Peres J-G, Dalier V (2021) Irradiated UAmO₂
368 transmutation discs analyses: from dissolution to accurate isotopic analyses. *J*
369 *Radioanal Nucl Chem* To be subm:To be submitted
- 370 5. Bourgeois M, Isnard H, Gourgiotis A, Stadelmann G, Gautier C, Mialle S,
371 Nonell A, Chartier F (2011) Sm isotope composition and Sm/Eu ratio
372 determination in an irradiated ¹⁵³Eu sample by ion exchange chromatography-
373 quadrupole inductively coupled plasma mass spectrometry combined with
374 double spike isotope dilution technique. *J Anal At Spectrom* 26:1660–1666.
375 <https://doi.org/10.1039/c1ja10070j>
- 376 6. Chartier F, Aubert M, Pilier M (1999) Determination of Am and Cm in spent
377 nuclear fuels by isotope dilution inductively coupled plasma mass spectrometry
378 and isotope dilution thermal ionization mass spectrometry after separation by
379 high-performance liquid chromatography. *Fresenius J Anal Chem* 364:320–327
- 380 7. Beattie P (1993) Uranium-thorium disequilibria and partitioning on melting of
381 garnet peridotite. *Nature* 363:63–65. <https://doi.org/10.1038/363063a0>
- 382 8. Condomines M, Allegre CJ (1976) Evidence for contamination of recent
383 Hawaiian lavas from ²³⁰Th-²³⁸U data. *Earth Planet Sci Lett* 33:122–125.
384 [https://doi.org/10.1016/0012-821X\(76\)90165-5](https://doi.org/10.1016/0012-821X(76)90165-5)

- 385 9. Condomines M, Hemond C, Allègre CJ (1988) UThRa radioactive disequilibria
386 and magmatic processes. *Earth Planet Sci Lett* 90:243–262.
387 [https://doi.org/10.1016/0012-821X\(88\)90129-X](https://doi.org/10.1016/0012-821X(88)90129-X)
- 388 10. Jia GD, Chabaux F, Van der Woerd J, Pelt E, di Chiara Roupert R, Ackerer J,
389 Zhao ZQ, Yang Y, Xu S, Liu CQ (2021) Determination of regolith production
390 rates from ^{238}U - ^{234}U - ^{230}Th disequilibrium in deep weathering profiles
391 (Longnan, SE China). *Chem Geol* 574:.
392 <https://doi.org/10.1016/j.chemgeo.2021.120241>
- 393 11. Shao QF, Li CH, Huang MJ, Liao ZB, Arps J, Huang CY, Chou YC, Kong XG
394 (2019) Interactive programs of MC-ICPMS data processing for $^{230}\text{Th}/\text{U}$
395 geochronology. *Quat Geochronol* 51:43–52.
396 <https://doi.org/10.1016/j.quageo.2019.01.004>
- 397 12. Ghaleb B, Falguères C (2017) Apport des méthodes basées sur le déséquilibre
398 radioactif (^{238}U - ^{234}U - ^{230}Th - ^{226}Ra - ^{210}Pb) aux études des variations et
399 changements climatiques. *Anthropol* 121:73–81.
400 <https://doi.org/10.1016/j.anthro.2017.03.008>
- 401 13. Mayer K, Wallenius M, Lützenkirchen K, Horta J, Nicholl A, Rasmussen G,
402 Van Belle P, Varga Z, Buda R, Erdmann N, Kratz JV, Trautmann N, Fifield
403 LK, Tims SG, Fröhlich MB, Steier P (2015) Uranium from German Nuclear
404 Power Projects of the 1940s - A Nuclear Forensic Investigation. *Angew*
405 *Chemie - Int Ed* 54:13452–13456. <https://doi.org/10.1002/anie.201504874>
- 406 14. Quemet A, Maillard C, Ruas A (2015) Determination of zirconium isotope
407 composition and concentration for nuclear sample analysis using Thermal
408 Ionization Mass Spectrometry. *Int J Mass Spectrom* 392:34–40.
409 <https://doi.org/10.1016/j.ijms.2015.08.023>
- 410 15. Quemet A, Ruas A, Esbelin E, Dalier V, Rivier C (2019) Development and
411 comparison of two high accuracy methods for uranium concentration in nuclear
412 fuel: ID-TIMS and K-edge densitometry. *J Radioanal Nucl Chem* 321:997–
413 1004. <https://doi.org/10.1007/s10967-019-06670-y>

- 414 16. Quemet A, Ruas A, Dalier V, Rivier C (2018) Americium isotope analysis by
415 Thermal Ionization Mass Spectrometry using the Total Evaporation Method.
416 Int J Mass Spectrom 431:8–14. <https://doi.org/10.1016/j.ijms.2018.05.017>
- 417 17. Vogl J (2007) Characterisation of reference materials by isotope dilution mass
418 spectrometry. J Anal At Spectrom 22:475–492.
419 <https://doi.org/10.1039/b614612k>
- 420 18. Rodríguez-González P, Ignacio García Alonso J (2019) Mass spectrometry |
421 Isotope dilution mass spectrometry. Encycl Anal Sci 6:411–420.
422 <https://doi.org/10.1016/B978-0-12-409547-2.14387-2>
- 423 19. Rudge JF, Reynolds BC, Bourdon B (2009) The double spike toolbox. Chem
424 Geol 265:420–431. <https://doi.org/10.1016/j.chemgeo.2009.05.010>
- 425 20. Désenfant M, Priel M (2017) Reference and additional methods for
426 measurement uncertainty evaluation. Measurement 95:339–344
- 427 21. Eaton JW (2012) GNU Octave and reproducible research. J Process Control
428 22:1433–1438. <https://doi.org/10.1016/j.jprocont.2012.04.006>
- 429 22. Quemet A, Angenieux M, Ruas A (2021) Nd, Am and Cm isotopic
430 measurement after simultaneous separation in transmutation irradiated samples.
431 J Anal At Spectrom 36:1758. <https://doi.org/10.1039/D1JA00165E>
- 432 23. Esbelin E (2014) Graphite monochromator for actinide L-line energy
433 dispersive X-ray fluorescence analysis in liquid sample. X-Ray Spectrom
434 43:198–208. <https://doi.org/10.1002/xrs.2540>
- 435 24. International Atomic Energy Agency (2010) International Target Values 2010
436 for Measurement Uncertainties in Safeguarding Nuclear Materials - STR368.
437 Vienna, Austria

438